SLIP-LINE FIELD SOLUTION WITH DEAD ZONE FOR LARGE NEGATIVE RAKE CUTTING

by

MINASSE ABEBE

B.S., Addis Abeba University, 1972

A MASTER'S THESIS

submitted in partial fulfillment of the
requirements for the degree

MASTER OF SCIENCE

Department of Mechanical Engineering

Kansas State University
Manhattan, Kansas

1980

Approved by:

F. C. Appl

Major Professor

THIS BOOK
CONTAINS
NUMEROUS PAGES
WITH THE ORIGINAL
PRINTING BEING
SKEWED
DIFFERENTLY FROM
THE TOP OF THE
PAGE TO THE
BOTTOM.

THIS IS AS RECEIVED
FROM THE
CUSTOMER.

TABLE OF CONTENTS

TABLE OF CONTENTS - Continued

LIST OF TABLES

LIST OF FIGURES

LIST OF FIGURES - Continued

LIST OF FIGURES - Continued

NOMENCLATURE

α	Negative rake angle
D	Depth of cut
W	Width of cut
d	Chip thickness
U	Workpiece velocity
U_{PC}, U_{GH}, etc.	Velocities in the Hodograph
U^*_{EG}, U^*_{DC}, etc.	Velocity discontinuities in the Hodograph
Y'	Yield stress in pure uniaxial tension
k,K	Yield stress in pure shear
α-Line	Slip-line of the family denoted by the parameter ϕ
β-Line	Slip-line of the family denoted by the parameter $(\phi+\pi/2)$
$\eta, \eta_1, \eta_2, \eta_3$	Friction angles; the angles between slip-lines and interfaces
R	Radius of the centered fan field PED
d_o	Height of chip formation, length HL in Fig. 4.1
$\phi, \phi_{10}, \phi_{12}$	The counter-clockwise angle of an α-line from the positive x-axis
$\theta, \theta_6, \theta_8$	The counter-clockwise angle of an α-line from the positive x-axis
$\sigma_x, \sigma_y, \sigma_z, \sigma, \sigma_n$	Normal stresses
$\sigma_1, \sigma_2, \sigma_3$	Principal normal stresses
$\tau_{xy}, \tau_{yx}, \tau$	Shear stresses
p	Hydrostatic stresses

$P_1, P_2, \ldots$etc.]
$P_a, P_b, P_v, P_v', P_7'$] Compressive normal stresses

$s_1, s_2, \ldots$etc.]
s_a, s_b, s_v, s_v'] Shear stresses

$P_3{}^D, P_{13}{}^D, P_{BC}{}^D, P_{va}{}^D$ Dimensionless compressive normal stresses

$s_3{}^D, S_{13}{}^D, S_{BC}{}^D, S_{va}{}^D$ Dimensionless shear stresses

FH — Horizontal component of the cutting force

FV — Vertical component of the cutting force

VOH — Ratio of the vertical component of the cutting force to the horizontal component of the cutting force

FT — Component of the cutting force normal to the tool face

FN — Component of the cutting force parallel to the tool face

FTD, FHD, FVD — Dimensionless components of cutting force; parallel to the tool face, horizontal and vertical, respectively.

PMOK — Dimensionless mean pressure on the tool face

X, x — Coordinate direction parallel to the tool face

Y, y — Coordinate direction normal to the tool face

ΣFy — Summation of forces in Y-direction

ΣFx — Summation of forces in X-direction

ΣM_o — Summation of moment about 0 in Fig. 4.4

m — Adhesion coefficient

μ — Friction coefficient

AR — Real area of contact

β_1, β_2 — Parameters in the Equation for AR

ξ — Parameter in the Equation for $\left(\frac{\sigma n}{2k}\right)_{lim}$

V_x, V_y — Velocity Components in X and Y directions

1.0 INTRODUCTION

Machining is an important metal removal process in manufacturing. However, the mechanics of this process are not fully understood. In the past, theoretical studies of metal cutting with positive rake angle tools have been conducted. Various theories have been presented, e.g., Merchant [1], Lee and Shaffer [5] and Hill [6]. But, on the nature of the cutting process with large negative rake angles very little published literature is available. Even if high negative rakes for single point cutting tools are rarely used, it is necessary to understand the cutting mechanisms at such rakes. Negative rakes exist in cutting with grinding grits, at the nose radius of a single point tool and in drilling rocks with diamond drill bits.

Rubenstein et al. [11] conducted experiments with large negative rake tools and concluded that chip formation ceases at about -55 deg. rake in machining both aluminum and 70:30 brass. They also observed that at higher negative rake angles the workpiece material flows sideways instead of up the rake face.

Rowe and Wetton [13] applied the slip-line field theory to the problem of indenting by a symmetrical truncated wedge. Their theory predicts first the formation of a frontal bulge (prow) which later transforms to a chip. The formation of the prow was experimentally proved.

Komanduri [14] conducted experiments in machining with a wide range of negative rake tools. He observed that it is possible to

obtain chips with as high a negative rake as -75 deg. At -85 deg. rake no chip was formed but the tool rubbed the work material causing considerable side flow. He also concluded that the ratio of the thrust force to cutting force is greater than 1 for high negative rakes. His other observations were that the force parallel to the rake face becomes zero at -76 deg. rake, and that a prow formed ahead of the cutting edge.

Abdelmoneim and Scrutton [28] conducted experiments with rake angles ranging from -55 deg. to -80 deg. in machining non-ferrous materials. One experimental observation was that no chip formed when using tools of -80 deg. rake.

Yoshihiro Kita et al [27] studied the mechanism of metal removal with a conic abrasive tool. They observed a stagnant region ahead of the tool face during cutting. Besides they found a relationship between the stagnant region and chip formation. If the position of the stagnant tip is under the surface of the workpiece the chip can be formed; but if the position of the stagnant tip is above the surface of the workpiece no chip will be produced.

Challen and Oxley [31] used slip-line field analysis to explain the deformation of a soft asperity by a hard one, the hard one being a negative rake model. They derived equations for wear rates and coefficients of friction.

Hein [35] developed an approximate slip-line field for a negative rake angle cutting problem. His solution was an upper bound type. His conclusion was that slip-line field theory can be applied to problems of cutting with large negative rake angle tools.

Yoshihiro Kita et al. [36] studied experimentally the cutting mechanism with large negative rake tools. In their experiments they tried to simulate plane strain in cutting. They observed a stagnant region ahead of the tool face. The size of this region increases as the rake angle becomes more negative. In their conclusions they noted that the ratio of the vertical force to the horizontal force is greater than 1.

Most of the research done on negative rake angle cutting has been experimental. The objective of the study conducted here is to develop a theory of the mechanics of cutting with large negative rake angle tools. As a basis for this study, the slip-line method, which has been successfully used in solving problems related to other types of metal forming processes is used. In developing the slip-line field, the formation of the prow and the stagnant region ahead of the tool, which have been experimentally demonstrated are considered. Using this method, from the given rake angle, type of material and depth of cut, the theoretical forces are calculated and are compared with available experimental results.

2. THEORY OF PLANE STRAIN PLASTIC DEFORMATION [21, 32, 34]

2.1 Conditions and Assumptions

There are many cutting processes, like orthogonal machining in which the depth of cut is relatively small compared to the width of cut, so that permanent deformation occurs in plane strain. Plane plastic deformation implies that the displacements of elements in the plastically deforming region all occur in parallel planes, for instance the X - Y plane, and are independent of the Z co-ordinate.

The workpiece material is assumed to be homogeneous and isotropic. In any plane, Z=constant, the same stress-strain relationship is applicable; the components of stresses depend only on X and Y, and τ_{xz}, τ_{yz} are zero. Thus the Z-direction is a principal direction and σ_z is a principal stress.

The elastic strains which must occur before the material is sufficiently stressed to become plastic are ignored. In such cases it is reasonable to assume that the workmaterial has an infinite Young's modulus of elasticity.

In the plastically deforming region of the workpiece strain-hardening is neglected so that the material is assumed to flow at constant yield stress. This material is referred to as rigid-perfectly plastic. The strain-rate at each point in the deforming region is usually different. The effect this may have on the yield stress is therefore ignored. During deformation involving high values of strain, most of the external energy used is dissipated as heat. Temperature gradients that can arise may affect the material properties; but this effect is neglected.

The slip-line method, which is based on plane strain plastic deformation, requires several assumptions that may not agree with the physical phenomenon it attempts to describe. However, many problems of real importance have been solved [20] which show good agreement with

experiment and theory.

2.2 Basic Plane Strain Equations

It can be shown for plane strain deformation in the X - Y plane

$$\sigma_z = \frac{\sigma_x + \sigma_y}{2} = p \quad \text{and} \quad \tau_{xz} = \tau_{yz} = 0 \tag{2.1}$$

The maximum shear stress in the plane flow is expressed as

$$\tau_{max} = \frac{\sigma_1 - \sigma_3}{2} = K \tag{2.2}$$

or

$$\tau_{max} = \left[\left(\frac{1}{4}\right) (\sigma_x - \sigma_y)^2 + \tau_{xy}^2 \right]^{\frac{1}{2}} \tag{2.3}$$

The principal stresses are

$$\sigma_1 = p + K, \; \sigma_2 = \sigma_z = p, \quad \text{and} \; \sigma_3 = p - K \tag{2.4}$$

Assuming the von-Mises yield criterion, the yield occurs when the maximum shear attains the value

$$K = Y'/\sqrt{3} \text{ , where } Y' \text{ is the yield stress in tension.} \tag{2.5}$$

The differential equations of equilibrium of forces for plane strain deformation in the X - Y plane, neglecting body and inertia forces are

$$\frac{\partial \sigma_x}{\partial x} + \frac{\partial \tau_{yx}}{\partial y} = 0 \tag{2.6}$$

$$\frac{\partial \tau_{xy}}{\partial x} + \frac{\partial \sigma_y}{\partial y} = 0 \tag{2.7}$$

Equations (2.3), (2.6), and (2.7) represent three equations with three unknowns. If the boundary conditions are stated only in terms of stresses, the above equations are sufficient to define the stress distribution independent of strain. This type of problem is referred to as being statically determinate. However, if displacements or velocities are specified over part of the boundary, the stress-strain equations may have

to be employed, and the problem becomes more complicated.

For the plane strain case, writing the strain rates in terms of velocities, we have for the requirement of constant volume (incompressiblity)

$$\frac{\partial V_x}{\partial x} + \frac{\partial V_y}{\partial y} = 0 \qquad (2.8)$$

The Saint Venant - von Mises plasticity relations can be re-arranged to give

$$\frac{\sigma_x - \sigma_y}{2\tau_{xy}} = \frac{\partial V_x/\partial x - \partial V_y/\partial y}{\partial V_x/\partial y + \partial V_x/\partial x} \qquad (2.9)$$

This states that the direction of the surface of maximum tangential stress coincides with the direction of the surface which experiences the maximum rate of shear strain.

So we have five equations (2.3), (2.6), (2.7), (2.8), and (2.9) for the five unknowns σ_x, σ_y, τ_{xy}, V_x, and V_y. This type of problem is referred to as statically indeterminate since the equations for stresses and velocities that have to be solved simultaneously are extremely difficult.

The state of stress at some point C in a plastically deforming region may be represented by the Mohr stress circle diagram as shown in Fig. 2.1.

The stresses σ_x, σ_y, and τ_{xy} can be expressed in terms of the hydrostatic pressure, p, and the yield shear stress, K, as follows

$$\begin{aligned} \sigma_x &= -p - K \operatorname{Sin} 2\phi \\ \sigma_y &= -p + K \operatorname{Sin} 2\phi \\ \pm\tau_{xy} &= \pm K \operatorname{Cos} 2\phi \end{aligned} \qquad (2.10)$$

2.3 Plain Strain Slip-Line Field Theory

2.3.1 Slip-Lines

The maximum shear stresses, $\tau_{max} = \pm K$ act on surfaces which make

THIS BOOK CONTAINS NUMEROUS PAGES WITH DIAGRAMS THAT ARE CROOKED COMPARED TO THE REST OF THE INFORMATION ON THE PAGE.

THIS IS AS RECEIVED FROM CUSTOMER.

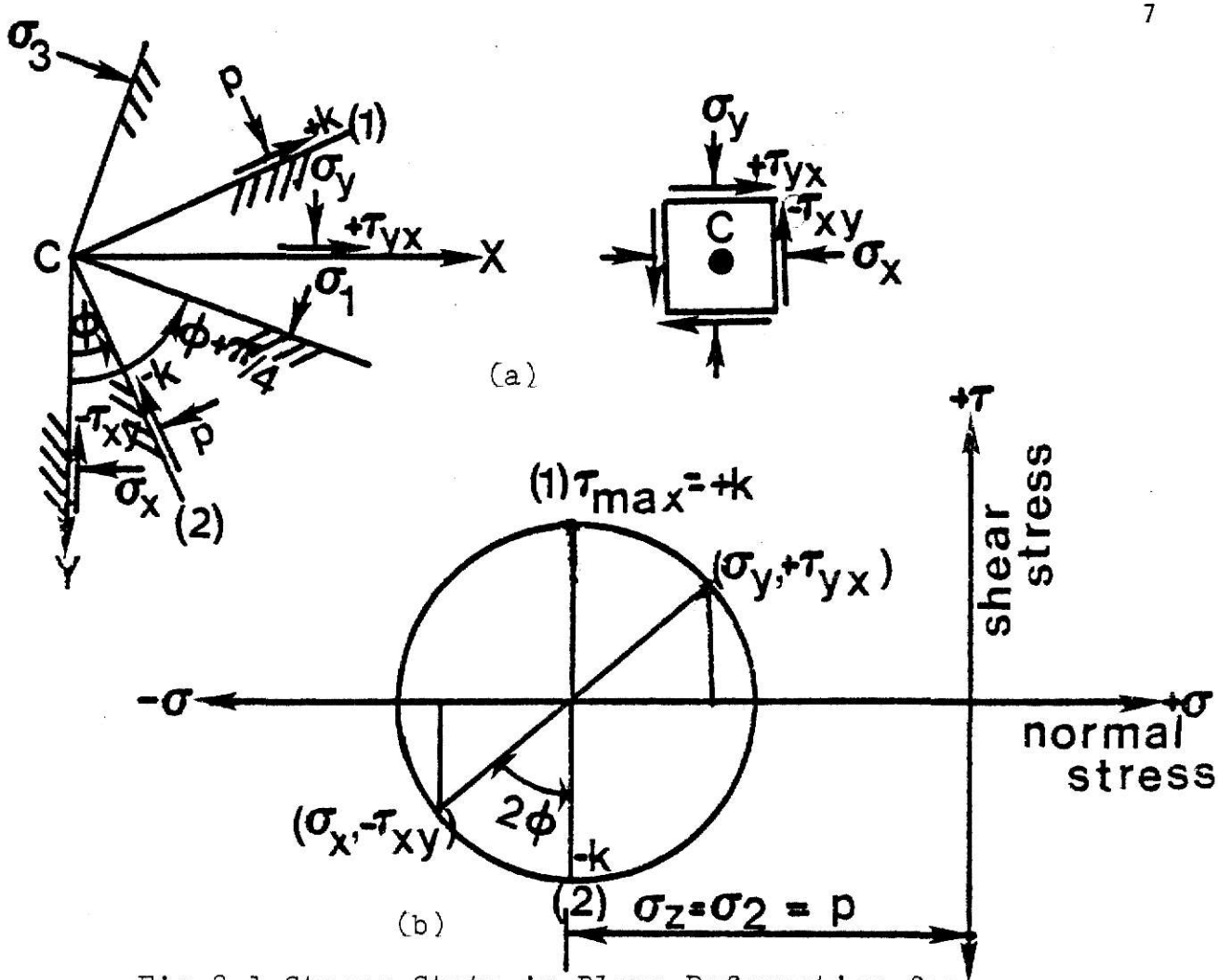

Fig.2.1.Stress State in Plane Deformation for a Rigid Perfectly Plastic Material Showing (a)the Physical Plane,and,(b)the Mohr Stress Circle Diagram.

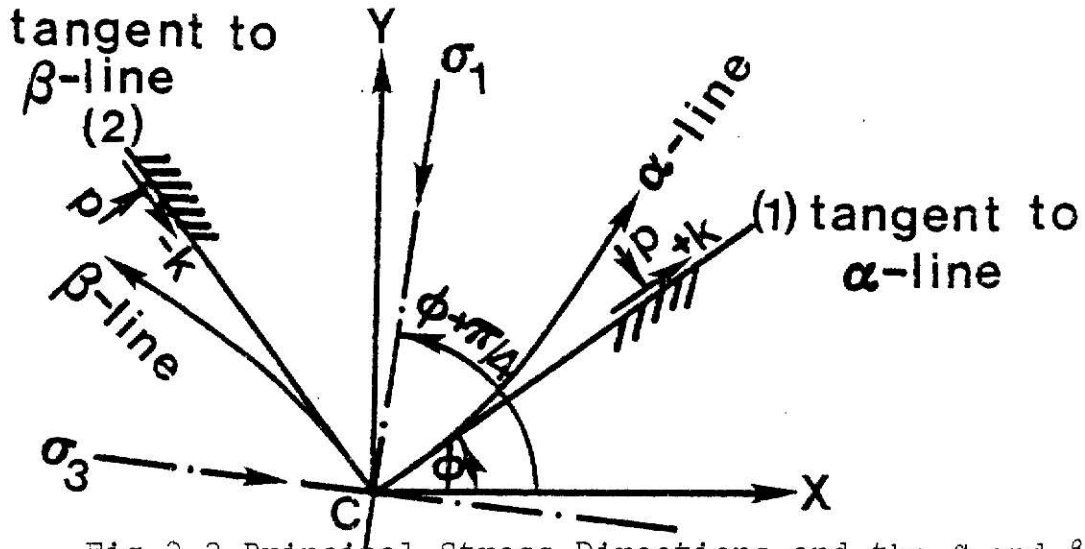

Fig.2.2.Principal Stress Directions and the α and β Directions at a Point in a Plastically Deforming Region.

angles of ±45° with the principal directions. If curves are drawn in the X - Y plane such that at every point on each curve the tangent coincides with the direction of maximum shear stress, then two orthogonal families of curves are obtained which are termed shear lines or slip lines. These two families of curves are usually designated as α-lines and β-lines. To distinguish between these two lines, the usual convention is that where the α and β-lines form a right-handed coordinate system of axes, then the line of action of the algebraic maximum principal stress, σ_1, as shown in Fig. 2.2 falls in the first and third quadrants. The anti-clockwise rotation, $\emptyset$, of the α-line from the chosen X-direction is then considered positive.

2.3.2 Hencky Stress Equations

The state of stress at a point can be expressed in terms of the independent quantities p, K and $\emptyset$ as in equations (2.10). Thus, the equilibrium equations (2.6) and (2.7) can be expressed in terms of these quantities as follows:

$$\begin{aligned} 2K \sin \emptyset \frac{\partial \emptyset}{\partial y} + \frac{\partial p}{\partial x} + 2K \cos 2\emptyset . \frac{\partial \emptyset}{\partial x} = 0 \\ 2K \sin \emptyset \frac{\partial \emptyset}{\partial x} + \frac{\partial p}{\partial y} - 2K \cos 2\emptyset . \frac{\partial \emptyset}{\partial y} = 0 \end{aligned} \qquad (2.11)$$

Equations (2.11) are the partial differential equations of equilibrium for the plane strain deformation of a rigid perfectly plastic material and are hyperbolic. The characteristics of the hyperbolic equations in this case, coincide with the slip lines.

The choice of X and Y axes is arbitrary. If we rotate the axes through $\emptyset$ such that the α and β lines coincide with the X, Y axes, $\emptyset$ becomes zero in equations (2.11) and as a result:

$$\frac{\partial p}{\partial x} + 2K\frac{\partial \phi}{\partial x} = 0$$

$$\frac{\partial p}{\partial y} - 2K\frac{\partial \phi}{\partial y} = 0 \qquad (2.12)$$

integrating (2.12), we have the Hencky equations

$$p + 2K\phi = C_1 \quad , \text{ along an } \alpha\text{-line}$$

$$p - 2K\phi = C_2 \quad , \text{ along a } \beta\text{-line} \qquad (2.13)$$

C_1 and C_2 are constants and their values generally vary from one slip-line to another.

2.3.3 Geiringer Velocity Equations

From Fig. 2.3 the velocity components in the X and Y directions are respectively

$$u_x = u \cos \phi - v \sin \phi$$
$$v_y = v \cos \phi + u \sin \phi \qquad (2.14)$$

Differentiating with respect to x and y respectively, and rotating the X - Y axes through ϕ so that the X-axis coincides with the α-line, that is, ϕ=0. We have

$$\frac{\partial u_x}{\partial x} = \frac{\partial u}{\partial x} - v\frac{\partial \phi}{\partial x}$$
$$\frac{\partial v_y}{\partial y} = \frac{\partial v}{\partial y} + u\frac{\partial \phi}{\partial y} \qquad (2.15)$$

Since the rate of extension along a slip-line is zero

$$\left(\frac{\partial u_x}{\partial x}\right)_{\phi=0} = \left(\frac{\partial v_y}{\partial y}\right)_{\phi=0} = 0 \qquad (2.16)$$

Thus equations (2.15) become:

$$du - v\,d\phi = 0 \quad \text{along an } \alpha\text{-line}$$
$$dv + u\,d\phi = 0 \quad \text{along a } \beta\text{-line} \qquad (2.17)$$

Equations (2.17) are the velocity compatiblity equations and are known as Geiringer's equations.

In many cases, it is possible to construct a graphical representation

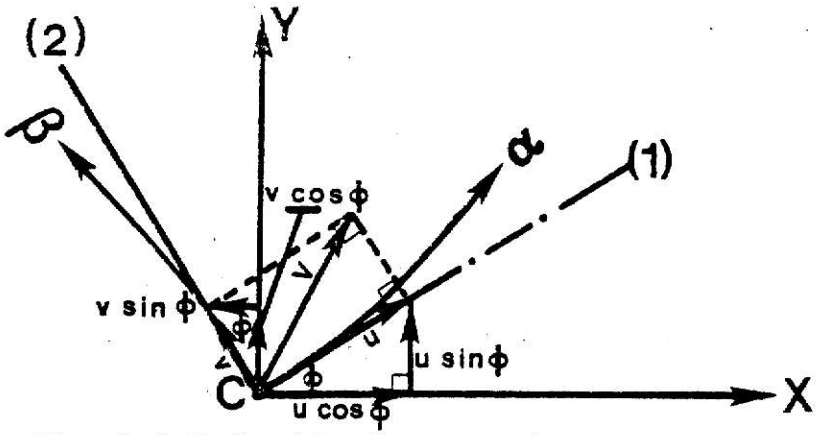

Fig.2.3.Velocity Components.

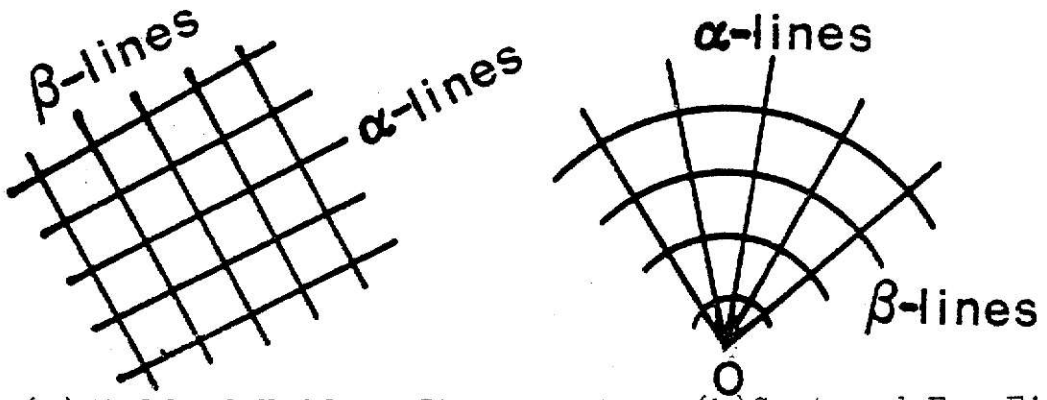

(a)Field of Uniform Stress. (b)Centered Fan Field.

Fig.2.4.Slip-Lines of Simple Stress States.

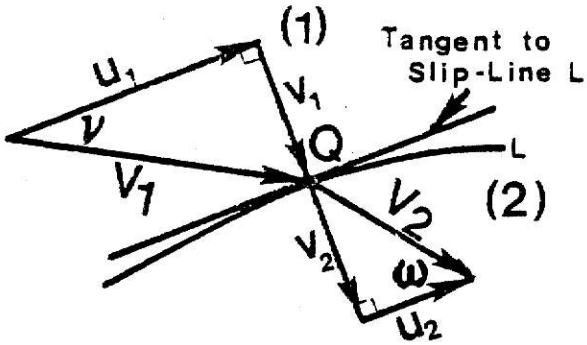

(a)Physical Plane.

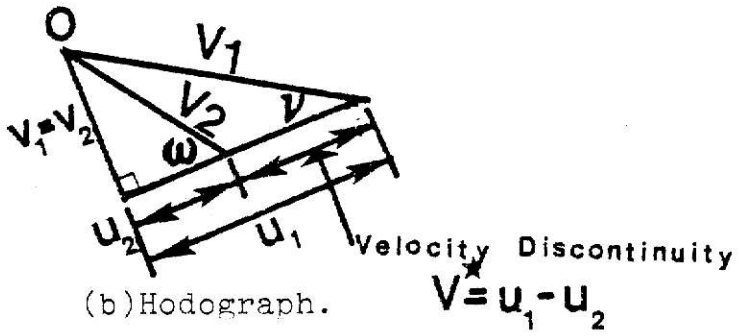

(b)Hodograph.

Fig.2.5.Velocity Discontinuity.

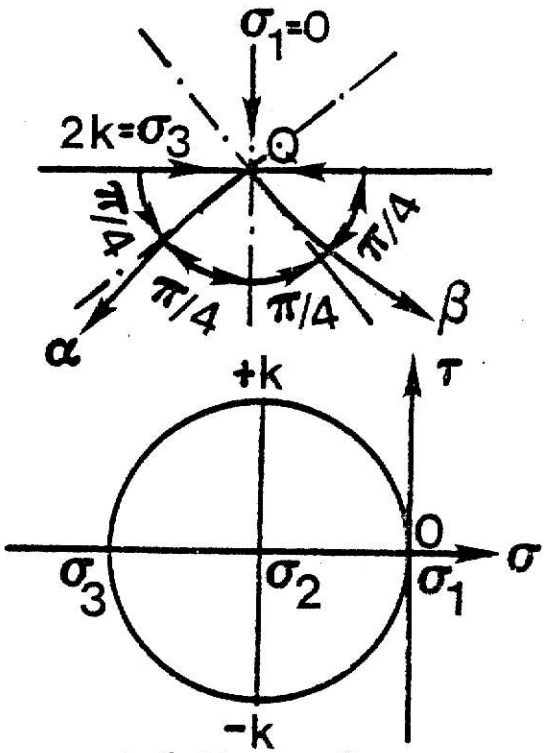

Fig.2.6.Stress Free Surface.

of the velocity at each point in a plastically deforming region. This is known as a hodograph The hodograph permits the evaluation of the magnitude and direction of the velocity at a point which is indicated as a vector.

2.3.4 Simple Stress-States

Fig. 2.4(a) shows a slip-line field generated by two orthogonal families of parallel straight lines. Using Hencky's stress equations (2.13) it can be shown that if the slip lines are straight then the angle, $\emptyset$, is constant along the slip lines and the hydrostatic pressure, p, remains constant. Also the stress components σ_x, σ_y, and σ_z must be constant. Thus the slip-line field of Fig. 2.4(a) represents a uniform stress state.

The slip-line field shown in Fig. 2.4(b) consists of a set of radial lines, say α-lines, intersected orthogonally by a set of concentric circular arcs, say β-lines. From the first of Hencky's stress equations (2.13), since $\emptyset$ is constant along an α-line, the hydrostatic pressure, p, must also be constant along an α-line. From the second of Hencky's stress equations, since $\emptyset$ varies linearly with distance along a β-line, the hydrostatic pressure, p, varies linearly with distance along a β-line. This type of slip-line field is known as the centered fan. The center of the fan, 0, is a point of stress singularity, and it can have any one of an infinite number of values.

In general a slip-line field can be constructed by combining both the uniform stress state and the centered fan fields.

2.3.5 Velocity Discontinuities

For a rigid-perfectly plastic material the displacements throughout the deforming material need not be continous. It is possible for there to be relative slipping between neighbouring zones in the deforming material.

The line of velocity discontinuity is a slip-line. As shown in Fig. 2.5(a) consider the material at Q crossing a slip-line. Let the material to the left of Q have a velocity V_1 with components v_1 and u_1 which are normal and tangential to the slip-line respectively. After crossing the slip-line its velocity changes to V_2 with corresponding components v_2 and u_2. Continuity at Q demands $v_1=v_2$; hence normal components of velocity when crossing a slip-line are always the same magnitude on either side of the slip line. However, it is possible for there to exist a velocity discontinuity of magnitude, $V^*=u_1-u_2$, tangential to the slip-line at the point Q, as shown in the hodograph in Fig. 2.5(b).

The magnitude of the tangential stress along a line of velocity discontinuity is equal to $\tau=\pm K$. In passing through such a line, an element experiences a finite shear in the direction in which the tangential stresses act and thus changes its direction of motion. The jump velocity, $V^*=u_1-u_2$ and the sense of the tangential stress, τ, are related by the condition that the plastic energy dissipation be positive: $\tau(u_1-u_2)>0$. Therefore, if the jump $V^*=u_1-u_2>0$, $\tau=+K$ and if $V^*=u_1-u_2<0$ then $\tau=-K$.

In general, once a velocity discontinuity is established across a slip-line there always exists a velocity discontinuity across any extension to the slip-line. Another general rule on slip-lines across which there is a discontinuity in the tangential component of velocity, is that, these slip-lines either form the boundary of the deforming region, or originate and/or terminate at a point of stress singularity within the field. These restrictions are necessary, otherwise compatibility of the velocity solution is violated.

2.3.6 Boundary Conditions for Stresses

2.3.6.1 Stress Free Surface

At a stress free surface there are no normal or shear components of

stress. The stress free surface is, therefore, a principal plane on which the principal stress is zero. It follows that the direction tangential to the free surface is a principal stress direction. The slip-lines indicate directions of maximum shear stress at anypoint in the material and intersect the free surface at angles of $\pm 45°$ as shown in Fig. 2.6(a).

The normal stress at the point Q can be considered as a zero compressive stress. Since the other principal stresses are also compressive and have greater magnitudes, the zero normal stress is the algebraic maximum principal stress, that is, $\sigma_1=0$. The algebraic minimum principal stress is $\sigma_3=-2K$. The Mohr's circle diagram is shown in Fig 2.6(b). The algebraic maximum principal stress, σ_1, has its direction contained in the first and third quadrants of the right-handed $\alpha-\beta$ co-ordinate system. Hence the α and β-lines are designated as shown in Fig. 2.6(a).

2.3.6.2 Friction Present at the Interface

At the tool-workpiece interface there can exist both shear and normal stresses. The shear stress tangential to the interface arises from friction conditions. If the magnitude of the shear and normal stresses are known the angle at which the family of slip-lines intersects the boundary can be found from the Mohr's circle as shown in Fig. 2.7(c). One slip-line will intersect the interface at some angle $\eta < 45°$. The determination of the magnitude of the shear and normal stress from a given friction condition will be discussed in Section 5.1.2.

In the case of no friction at the interface, the slip-lines intersect the interface at angles of $\eta = \pm 45°$. If the frictional stress becomes so high that the workpiece material will yield in shear at the interface, one slip-line meets the interface tangentially and the other normally. Under these conditions the interface is usually referred to as being perfectly rough.

2.3.7 Requirements for a Complete Solution

2.3.7.1 General Requirements

A complete solution to the plane strain deformation of a rigid-perfectly plastic material requires:

1. A statically admissible stress field which satisfies the equilibrium equations and the stress boundary conditions and nowhere is the yield criterion to be violated.

2. A kinematically admissible velocity field that is compatible with the stress field.

3. The rate of plastic work is everywhere positive.

4. The yield criterion is not violated in the material adjacent to the plastic region. That is, the material must be capable of supporting the stresses transmitted across the boundary without yielding.

2.3.7.2 Check of Positive Rate of Work

Plastic work is always positive, that is, work has to be done on materials to cause permanent deformation. It is necessary to check that any slip-line solution does not violate this fact at any point throughout the field.

The following method of verifying that the plastic energy dissipation be positive was suggested by Ford [33]. In Fig. 2.8(a), a curvilinear element ABCD is bounded by a pair of α and β-lines. The corresponding hodograph is shown in Fig. 2.8(b). The plastic energy dissipation in the element will be positive provided the velocity of C relative to A represented by the vector, $\overrightarrow{ac}$, in the hodograph is positive, that is, having a sense from A to C, and the velocity of D relative to B represented by the vector $\overrightarrow{bd}$ is positive, that is, having a sense from D to B corresponding with the sign of the shear stresses in the physical plane of Fig. 2.8(a).

Velocity discontinuities need to be considered separately. The jump

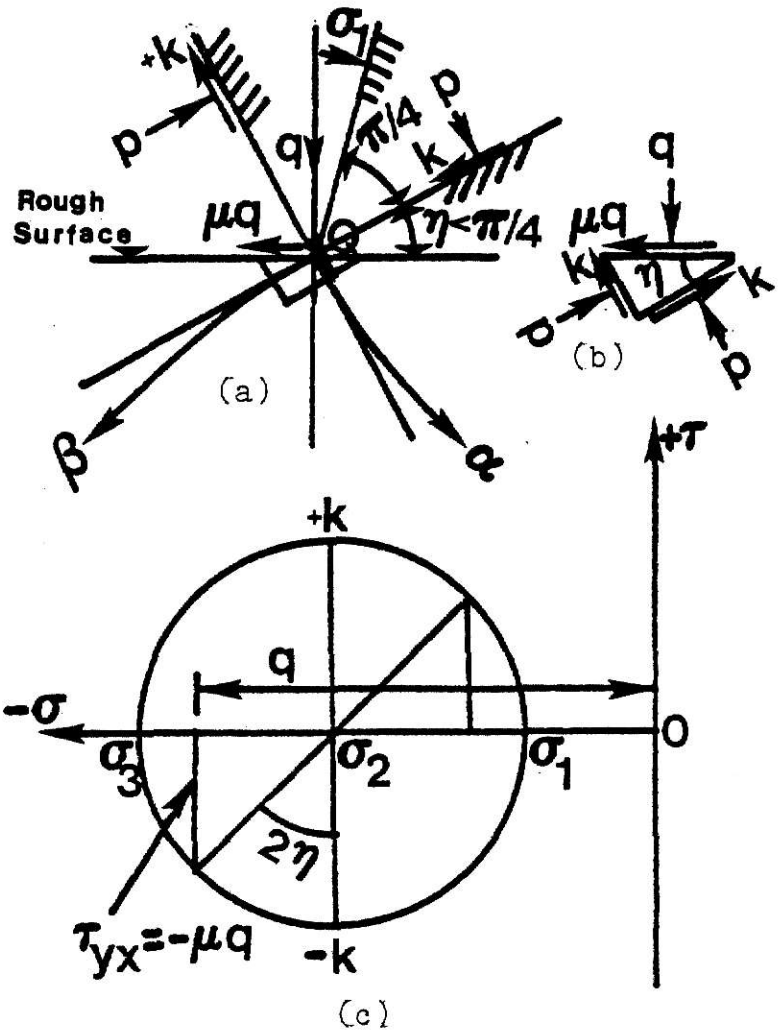

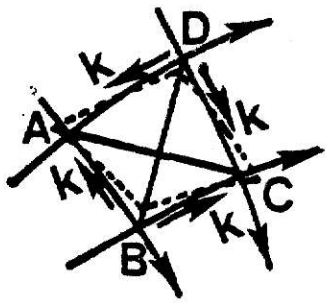

(a) Physical Plane

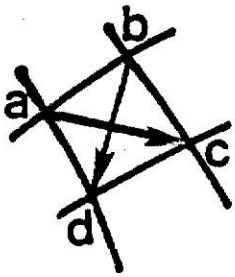

(b) Hodograph.

Fig.2.8.Verification of Positive Plastic Energy Dissipation.

Fig.2.7.Rough Surface,(a)Intersection of the Slip-Lines at Point Q in an Interface where Friction is Present (b)Stresses Acting on an Element, (c)Mohr Stress Circle Diagram.

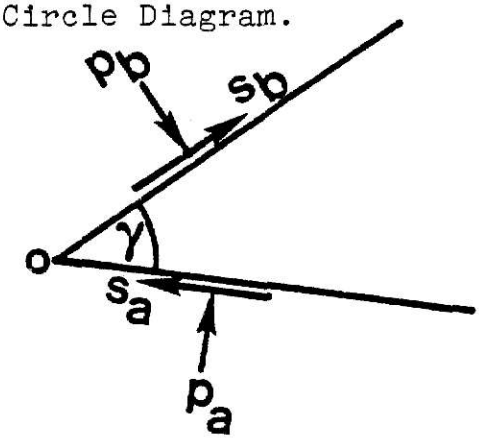

Fig,2.9. State of Stress at a Vertex.